Trapping Dirac fermions in tubes generated by two scalar fields

R. Casana,[1] A. R. Gomes,[2,*] G. V. Martins,[1] and F. C. Simas[1]

[1]*Departamento de Física, Universidade Federal do Maranhão, 65080-805 São Luís, Maranhão, Brazil*
[2]*Departamento de Física, Instituto Federal do Maranhão, 65025-001 São Luís, Maranhão, Brazil*

In this work we consider (1,1)-dimensional resonant Dirac fermionic states on tubelike topological defects. The defects are formed by rings in (2,1) dimensions, constructed with two scalar fields ϕ and χ, and embedded in the (3,1)-dimensional Minkowski spacetime. The tubelike defects are attained from a Lagrangian density explicitly dependent with the radial distance r relative to the ring axis and the radius and thickness of its cross section are related to the energy density. For our purposes we analyze a general Yukawa-like coupling between the topological defect and the fermionic field $\eta F(\phi, \chi)\bar{\psi}\psi$. With a convenient decomposition of the fermionic fields in left and right components, we establish a coupled set of first-order differential equations for the amplitudes of the left and right components of the Dirac field. After decoupling and decomposing the amplitudes in polar coordinates, the radial modes satisfy Schrödinger-like equations whose eigenvalues are the masses of the fermionic states. With $F(\phi, \chi) = \phi\chi$ the Schrödinger-like equations are numerically solved with appropriated boundary conditions. Several resonance peaks for both components are obtained, and the results are confronted with the qualitative analysis of the Schrödinger-like potentials.

I. INTRODUCTION

Braneworld scenarios have their origins in attempts to solve important problems of theoretical physics such as the cosmological constant and the gauge hierarchy [1–5]. In the original formulation of thin branes, the matter fields are by construction localized on a brane with energy density described by a delta function [6], while gravity propagates in all dimensions. The usual Newton's law can then be reproduced on the brane depending on the metric warp factor attained after solving Einstein's equations. Several extensions soon appeared, with smooth thick branes constructed by scalar fields [7–16]. A comprehensive review on this subject can be found in Ref. [17]. This opened up the idea of matter fields to visit extra-dimension space, with a possible signal of deviations of the standard model due to extra dimensions.

In general, thick branes are possibly able to trap gravitons and scalar fields. For fermions, however, the introduction of the fermion-scalar coupling is a necessary condition to ensure the normalizable zero modes. This is a known property already demonstrated by Jackiw and Rebbi [18] for domain walls. For some models, the massive fermionic states leak from the branes but stay for a sufficiently longer time to be characterized as resonances [19–27]. In particular, Ref. [28] analyzed the localization of matter fields in branes constructed from a scalar field coupled to a dilaton. In Ref. [29], the localization and mass spectra of various matter fields in a thick anti–de Sitter brane were investigated. For fermionic Kaluza-Klein modes, bound states for both

chiralities were found. In Ref. [23], some of the authors of the present work have investigated the presence of massive modes for right-hand and left-hand fermions with branes with internal structure constructed by two scalar fields coupled to gravity by introducing a simple Yukawa coupling.

In this work we are interested in topological defects embedded in a flat spacetime that can be constructed following a similar procedure used for modeling branes, namely, the embedding of a topological defect in one or more extra dimensions. Thus, inspired by the physics of extra dimensions, in Sec. II we consider (2,1)-dimensional ringlike topological defects [30,31] which are embedded in a (3,1)-dimensional flat spacetime forming a tubelike topological defect. In Sec. III, we study some aspects of localization of fermionic fields in this system. We have particular interest for resonance effects, which are studied in Sec. IV. Our conclusions are presented in Sec. V.

II. A TUBE IN (3,1) DIMENSIONS

A tube in (3,1) dimensions can be described by the action

$$S_{\text{tube}} = \int dt d^3 x \left(\frac{1}{2} \partial_A \phi \partial^A \phi + \frac{1}{2} \partial_B \chi \partial^B \chi - V(\phi, \chi) \right),\tag{1}$$

with

$$V(\phi, \chi) = \frac{1}{2r^2}(W_\phi^2 + W_\chi^2).\tag{2}$$

We use capital letters A, B, ... for all (3,1) dimensions. The explicit dependence of $r = \sqrt{y^2 + z^2}$ follows closely and

*Corresponding author.
argomes@ifma.edu.br

generalizes for two fields the construction of Refs. [30,31] for evading the Derrick-Hobart theorem [32–34].

We notice that this construction breaks translational invariance, which is also present in QCD scenarios. For instance, in investigations which deal with color super-conductivity, pairing with quarks with different chemical potentials results in crystalline quark matter condensates which spontaneously break translational and rotational invariance, and include spin-zero Cooper pairs [35,36]. In Refs. [37,38] the effective Lagrangian density describing the color-flavor locked symmetry phase of QCD at high density has fields depending on the velocity of the massless Dirac fermions. With the glueball effective Lagrangian model the breaking of Lorentz invariance induced by the quark chemical potential affects the critical temperature for the onset of the superconductive state [39]. The breaking of translational invariance also occurs in problems dealing with brane intersections [40,41], noncommutative field theory with nonconstant noncommutativity [42,43] and condensed matter physics [44,45].

The equations of motion for static solutions are

$$\frac{1}{r}\frac{d}{dr}\left(r\frac{d\phi}{dr}\right) = \frac{1}{r^2}(W_\phi W_{\phi\phi} + W_\chi W_{\chi\phi}), \qquad (3)$$

$$\frac{1}{r}\frac{d}{dr}\left(r\frac{d\chi}{dr}\right) = \frac{1}{r^2}(W_\phi W_{\phi\chi} + W_\chi W_{\chi\chi}). \qquad (4)$$

In this work we restrict ourselves to configurations with radial symmetry, i.e., the fields $\phi = \phi(r)$ and $\chi = \chi(r)$ depend only on r. One can show that the solutions of the first-order equations [30]

$$\frac{d\phi}{dr} = \frac{1}{r}W_\phi, \qquad \frac{d\chi}{dr} = \frac{1}{r}W_\chi \qquad (5)$$

are also solutions of the second-order equations (3) and (4). The change of variables $d\xi = (1/r)dr$ effectively turns the two-dimensional model into a one-dimensional one, since Eqs. (5) can be rewritten as

$$\frac{d\phi}{d\xi} = W_\phi, \qquad \frac{d\chi}{d\xi} = W_\chi. \qquad (6)$$

In this work, for generating the tube solution we consider [46]

$$W(\phi,\chi) = \lambda\left(\phi - \frac{1}{3}\phi^3 - s\phi\chi^2\right). \qquad (7)$$

This choice of $W(\phi,\chi)$ with the potential $\tilde{V}(\phi,\chi) = (1/2)(W_\phi^2 + W_\chi^2)$ was studied in Ref. [46]. The potential $\tilde{V}(\phi,\chi)$ has minima at $(\pm1,0)$ and $(0,\pm\sqrt{1/s})$ with $s > 0$ and the equations of motion have static solutions

connecting the minima $(\pm1,0)$ as defects with internal structure known as Bloch walls. The limit $s \to 0.5$ turns the two-field problem into a one-field model with a solution known as the Ising wall. See also Refs. [47,48] for other solutions. The extension of this construction to (4,1) dimensions leading to a Bloch brane was presented in Ref. [15]. The richer structure of degenerate and critical Bloch branes was proposed in Ref. [49]. In Ref. [15] it was shown that the presence of the field χ is crucial to giving internal structure to the brane. In the present work the presence of the field χ also contributes to generate an internal structure to the tube formed. We will see that this is crucial for localizing fermions with a simple Yukawa coupling.

The choice given by Eq. (7) generates the known one-dimensional solutions for Eqs. (6)

$$\phi(\xi) = \tanh(2\lambda s\xi),$$

$$\chi(\xi) = \pm\sqrt{\frac{1}{s} - 2}\operatorname{sech}(2\lambda s\xi), \qquad (8)$$

where $0 < s < 1/2$. Changing back to the r variable we get

$$\phi(r) = \tanh(2\lambda s \ln(r/r_0)),$$

$$\chi(r) = \pm\sqrt{\frac{1}{s} - 2}\operatorname{sech}(2\lambda s \ln(r/r_0)), \qquad (9)$$

which has a ring profile and r_0 can be identified with the ring radius of the tube's cross section.

The energy density of the two-dimensional defect is

$$T_{00} = \frac{(2\lambda s)^2}{r^2}\operatorname{sech}^4\left[2\lambda s \ln\left(\frac{r}{r_0}\right)\right]$$

$$\times \left\{1 + \left(\frac{1}{s} - 2\right)\sinh^2\left[2\lambda s \ln\left(\frac{r}{r_0}\right)\right]\right\}. \qquad (10)$$

Here we consider T_{00} finite in $r = 0$, which restricts the parameters to satisfy $\lambda s \geq \frac{1}{2}$ when $\lambda > 1$. Figures 1(a) and 1(b) depict the energy density $T_{00}(r)$ for fixed $r_0 = 1$ and several values of λ and coupling constant s. We note that for fixed $\lambda > 1$ and $\frac{1}{2\lambda} \leq s < \frac{1}{2}$, the behavior of the energy density changes from a lump centered in $r = 0$ ($s = \frac{1}{2\lambda}$) to a peak centered around r_0 ($s = \frac{1}{2}$). For fixed s, the maximum amplitude of T_{00} increases with λ, so large values of λ produce more interesting results. For large values of λ, there exists a value s_0 so that for $\frac{1}{2\lambda} < s < s_0$, the effects of the field χ are strong and the defect appears as a thick tube structure whose center is localized between the origin and r_0. On the other hand, for $s_0 \lesssim s < \frac{1}{2}$ it is clear the predominance of the field ϕ and the defect looks like a thin tube centered around r_0.

This means that for larger values of λ we can characterize the defect as a ring in the two-dimensional yz plane, or as a cylindrical tube in the three-dimensional space oriented
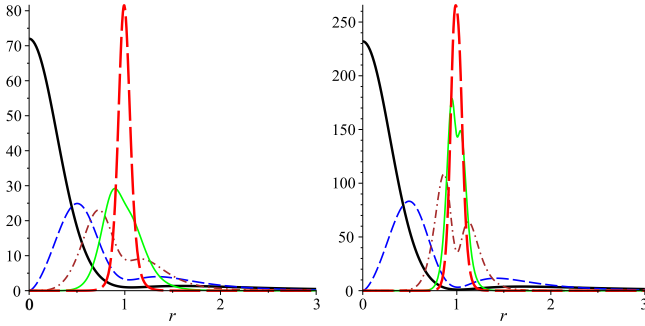
FIG. 1 (color online). Energy density $T_{00}(r)$ for $r_0 = 1$: (a) (left) $\lambda = 10$, $s = 0.05$ (black thick line), $s = 0.09$ (blue dashed thin line), $s = 0.15$ (brown dash-dotted thin line), $s = 0.25$ (green thin line), $s = 0.45$ (red long-dashed thick line). (b) (right) $\lambda = 30$, $s = 1/60$ (black thick line), $s = 0.03$ (blue dashed thin line), $s = 0.1$ (brown dash-dotted thin line), $s = 0.2$ (green thin line), $s = 0.27$ (red long-dashed thick line).

along the symmetry x axis. The influence of larger values of s shows that the χ field is responsible for the process of generating a thicker tube. The total energy in the yz plane is given by $E = 8\pi\lambda/3$, which can be identified with the mass of the ring, M_{ring}.

III. FERMION LOCALIZATION

We are interested in the localization of (1,1)-dimensional fermions in an infinite tube whose transversal section is the two-dimensional ring. Here, the tube in consideration is the one analyzed in the previous section. In considering fermionic states on a tubelike defect, we must remark that the analysis about the existence or not of fermionic zero modes was also considered in the other contexts. One can cite fermions in the field of Abelian and non-Abelian [50–52] vortex solutions and more specifically neutrino zero modes on electroweak strings [53–55].

In the following we consider the fermionic field coordinates as $(x^0, x^1) = (t, x)$ and the ring coordinates as $(x^2, x^3) = (y, z)$. Then, after neglecting the backreaction on the tube, we consider the following fermionic action

$$S_{\text{ferm}} = \int dt dx dy dz [\bar{\Psi}\Gamma^A \partial_A \Psi - \eta F(\phi, \chi)\bar{\Psi}\Psi], \quad (11)$$

where the Γ^0, Γ^1 matrices are defined as

$$\Gamma^0 = i\gamma^0 = i\sigma^1, \qquad \Gamma^1 = i\gamma^1 = \sigma^2, \quad (12)$$

and Γ^2, Γ^3 are conveniently chosen to provide Schrödinger's equations in the yz plane whose potentials are supersymmetric partners. Here $F(\phi(r), \chi(r)) = F(r)$ is a function of the scalar fields $\phi(r)$ and $\chi(r)$ giving the ring solution in Eqs. (9) and η is the coupling constant.

An important point to note is that in (3,1) dimensions, usually the Dirac spinors and gamma matrices are

four-component objects. However, owing to the cylindrical symmetry of the tube, there occurs an effective dimensional reduction to a (2,1) theory, and the Dirac spinors and matrices can be taken with only two components. This is a well-known procedure in dealing with vortex problems since the seminal work of Jackiw and Rossi [52]. A similar procedure was made by Witten in the context of superconducting strings [56].

After transforming the yz plane to polar coordinates, the equation of motion for Ψ is found as

$$i\gamma^\mu \partial_\mu \Psi + \begin{pmatrix} \partial_r + \frac{i}{r}\partial_\theta & 0 \\ 0 & -\left(\partial_r - \frac{i}{r}\partial_\theta\right) \end{pmatrix} \Psi - \eta F\Psi = 0,$$

$$(13)$$

where greek letters $\mu, \nu \ldots$ are for the (t, x) coordinates and we have chosen

$$\Gamma^r = \sigma^3 = \begin{pmatrix} 1 & 0 \\ 0 & -1 \end{pmatrix}, \qquad \Gamma^\theta = i1 = \begin{pmatrix} i & 0 \\ 0 & i \end{pmatrix}. \quad (14)$$

We decouple the coordinates (t, x) from (r, θ) by making the decomposition

$$\Psi(t, x, y, z) = \sum_n \begin{pmatrix} R_n(r, \theta)\Psi_{Rn}(t, x) \\ L_n(r, \theta)\Psi_{Ln}(t, x) \end{pmatrix}, \quad (15)$$

and by imposing that Ψ_{Rn} and Ψ_{Ln} are the components of a massive fermion satisfying the $(1 + 1)$-dimensional Dirac equation

$$(i\gamma^\mu \partial_\mu - M_n)\psi_n = 0, \qquad \psi_n = \begin{bmatrix} \Psi_{Rn} \\ \Psi_{Ln} \end{bmatrix}, \quad (16)$$

we can rewrite Eq. (13) in the following set of equations for the amplitudes $L_n(r, \theta)$ and $R_n(r, \theta)$:

$$\left(\partial_r - \frac{i}{r}\partial_\theta\right) L_n + \eta F L_n = M_n R_n, \quad (17)$$

$$-\left(\partial_r + \frac{i}{r}\partial_\theta\right) R_n + \eta F R_n = M_n L_n. \quad (18)$$

Now we make the useful decomposition

$$L_n(r, \theta) = \sum_\ell \Lambda_{n\ell}(r)e^{i\ell\theta}, \quad (19)$$

$$R_n(r, \theta) = \sum_\ell \varrho_{n\ell}(r)e^{i\ell\theta}, \quad (20)$$

where $\ell \in \mathbb{Z}$ and the functions $\Lambda_{n\ell}, \varrho_{n\ell}$ are finite in $r = 0$. Other decompositions are used in other contexts, see for instance, Refs. [57–59].

By combining Eqs. (17) and (18) we attain the Schrödinger-like equations for the scalar modes $\Lambda_{n\ell}(r)$ and $\varrho_n(r)$

$$-\frac{d^2\Lambda_{n\ell}}{dr^2} + V_{\text{sch}}^L(r)\Lambda_{n\ell} = \hat{H}_{\text{sch}}^L\Lambda_{n\ell} = M_n^2\Lambda_{n\ell}, \quad (21)$$

$$-\frac{d^2\varrho_{n\ell}}{dr^2} + V_{\text{sch}}^R(r)\varrho_{n\ell} = \hat{H}_{\text{sch}}^R\varrho_{n\ell} = M_n^2\varrho_{n\ell}, \quad (22)$$

where the potentials are given by

$$V_{\text{sch}}^L(r) = \frac{\ell(\ell+1)}{r^2} + 2\eta\ell\frac{F}{r} - \eta(\partial_r F) + \eta^2 F^2, \quad (23)$$

$$V_{\text{sch}}^R(r) = \frac{\ell(\ell-1)}{r^2} + 2\eta\ell\frac{F}{r} + \eta(\partial_r F) + \eta^2 F^2. \quad (24)$$

Then, we have transformed the equation for fermions in a set of independent Schrödinger-like equations for the amplitudes $\Lambda_{n\ell}$ and $\varrho_{n\ell}$ allowing us to get our goal of finding massive modes and analyzing their localization properties. Equations (21) and (22) allow us to adopt a probabilistic interpretation for finding massive modes of both components in the tube. Here we are mainly interested in resonant states.

The Hamiltonians defining the Schrödinger-like equations (21) and (22) can be rewritten in terms of the conjugate operators $\hat{A}$ and $\hat{A}^\dagger$

$$\hat{A} = \frac{d}{dr} + \frac{\ell}{r} + \eta F, \qquad \hat{A}^\dagger = -\frac{d}{dr} + \frac{\ell}{r} + \eta F, \quad (25)$$

as being $\hat{H}_{\text{sch}}^L = \hat{A}^\dagger\hat{A}$ and $\hat{H}_{\text{sch}}^R = \hat{A}\hat{A}^\dagger$ guaranteeing the eigenvalues m_n^2 to be non-negative. In this way it is forbidden the existence of tachyonic modes.

Since Eqs. (21) and (22) form a couple of Sturm-Liouville systems, the eigenfunctions $\Lambda_{n\ell}$ and $\varrho_{n\ell}$, respectively, establish a complete set of orthonormal functions satisfying

$$\int_0^\infty dr\Lambda_{m\ell}\Lambda_{n\ell} = \delta_{mn}, \quad (26)$$

$$\int_0^\infty dr\varrho_{m\ell}\varrho_{n\ell} = \delta_{mn}. \quad (27)$$

Further note that the action S_{ferm} given by Eq. (11) can be integrated in the (y,z) dimensions in order to obtain an action for the left and right components of the Dirac fermions

$$S_{\text{ferm}} = \int dtdx\sum_{m,n}C_{mn}\Psi_{Lm}^*[i(\partial_0 - \partial_1)\Psi_{Ln} - M_n\Psi_{Rn}]$$

$$+ \int dtdx\sum_{m,n}D_{mn}\Psi_{Rm}^*[i(\partial_0 + \partial_1)\Psi_{Rn} - M_n\Psi_{Ln}], \quad (28)$$

where we have defined the symmetric matrices

$$C_{mn} = 2\pi\sum_\ell\int_0^\infty drr\Lambda_{m\ell}\Lambda_{n\ell}, \quad (29)$$

$$D_{mn} = \sum_\ell 2\pi\int_0^\infty drr\varrho_{m\ell}\varrho_{n\ell}. \quad (30)$$

In this way, the action given by Eq. (28) gives the equations of motion for the left and right components of ψ_n

$$i(\partial_0 - \partial_1)\Psi_{Ln} - M_n\Psi_{Rn} = 0, \quad (31)$$

$$i(\partial_0 + \partial_1)\Psi_{Rn} - M_n\Psi_{Ln} = 0, \quad (32)$$

as required in Eq. (16).

On the other hand, by requiring Hermiticity of the action (28) we attain to $C_{mn} = D_{mn}$ leading to

$$S_{\text{ferm}} = \int dtdx\sum_{m,n}C_{mn}[\bar{\psi}_m i\gamma^\mu\partial_\mu\psi_n - M_n\bar{\psi}_m\psi_n], \quad (33)$$

which after fermionic field redefinition represents an action describing a tower of Dirac's massive fermions.

Now we consider the issue of the existence of the zero-mode χ_0 which is obtained from

$$\hat{A}\chi_0 = 0. \quad (34)$$

For fixed ℓ the Hamiltonian H_{sch}^R is a quantum-mechanical supersymmetric partner of the Hamiltonian H_{sch}^L with superpotential

$$\mathcal{W} = \frac{\ell}{r} + \eta F, \quad (35)$$

hence the solution for the zero mode is

$$\chi_0 \propto r^{-\ell}\exp\left\{-\eta\int_0^r dr'F(r')\right\}. \quad (36)$$

In our analysis we are considering the Yukawa coupling, $F(\phi,\chi) = \phi(r)\chi(r)$. Hence, because the integral $\int_0^r dr'F(r')$ is finite for all r the zero mode is non-normalizable for all ℓ. Since the zero mode of H_{sch}^L is non-normalizable, we conclude that the spectra of H_{sch}^L and H_{sch}^R are identical due to the spontaneous breaking of supersymmetry in this quantum-mechanical system [60,61].

IV. NUMERICAL RESULTS

For our purposes we consider a simple Yukawa coupling, $F(\phi) = \phi\chi$. Interesting considerations for this and other couplings in models of two scalar fields can be found in Ref. [62].

The solutions compatible with $\langle\hat{A}f|g\rangle = \langle f|\hat{A}^\dagger g\rangle$ must be null in $r = 0$.

In order to investigate numerically the massive states, first we consider the region near the origin ($r \ll r_0$) where

$$F(r) \sim -2\sqrt{\frac{1}{s} - 2}\left(\frac{r}{r_0}\right)^{2\lambda s}. \qquad (37)$$

Then for $\lambda s \geq 1/2$, the functions F/r, $\partial_r F$ and F^2 are finite and the potentials $V^L_{\text{sch}}(r)$ and $V^L_{\text{sch}}(r)$ are dominated by the contributions of the angular momentum proportional to $1/r^2$. In this way, for the left component the potential is reduced to

$$\tilde{V}^L_{\text{sch}}(r) \approx \frac{\ell(\ell+1)}{r^2}. \qquad (38)$$

This gives that in the neighborhood of the origin we must have

$$\Lambda_{n\ell}(r) = \sqrt{r}J_{\ell+\frac{1}{2}}(m_n r), \qquad \ell \geq 0, \qquad (39)$$

$$\Lambda_{n\ell}(r) = \sqrt{r}Y_{\ell+\frac{1}{2}}(m_n r), \qquad \ell \leq -1. \qquad (40)$$

For the right component we have

$$\tilde{V}^R_{\text{sch}}(r) \approx \frac{\ell^2 - \ell}{r^2}, \qquad (41)$$

and from the same argument the solutions null in $r = 0$ are

$$\varrho_{n\ell}(r) = \sqrt{r}J_{\ell-\frac{1}{2}}(m_n r), \qquad \ell \geq 1, \qquad (42)$$

$$\varrho_{n\ell}(r) = \sqrt{r}Y_{\ell-\frac{1}{2}}(m_n r), \qquad \ell \leq 0. \qquad (43)$$

Hence, for each value of ℓ, Eqs. (39) and (40) or (42) and (43) are used as an input for the Runge-Kutta-Fehlberg method which produces a fifth-order accurate solution.

We now define the probability for finding fermions inside the tube of radius r_0 as in Ref. [24]

$$P_{\text{tube}} = \frac{\int_{r_{\min}}^{r_0} dr |\varphi_{n\ell}(r)|^2}{\int_{r_{\min}}^{r_{\max}} dr |\varphi_{n\ell}(r)|^2}, \qquad (44)$$

where $\varphi_{n\ell} = \Lambda_{n\ell}, \varrho_{n\ell}$. Here $r_{\min} \ll r_0$ is used as the initial condition and $r_{\max}$ is the characteristic box length used for the normalization procedure being a value where the Schrödinger potentials are close to zero and where the massive modes oscillate as plane waves.

From the energy density considerations after Figs. 1(a) and 1(b), larger values of λ favor the existence of a Schrödinger potential with structure similar to a tube barrier in $r = r_0$. Figure 2 depicts the Schrödinger-like potential $V^L_{\text{sch}}(r)$ and $V^R_{\text{sch}}(r)$ for $\ell = 2$, $\lambda = 30, 50$, and fixed $\eta = 30$ and $r_0 = 1$. The potentials in general diverge in $r \to 0$, assume a form of a barrier around $r = r_0$ and asymptote to
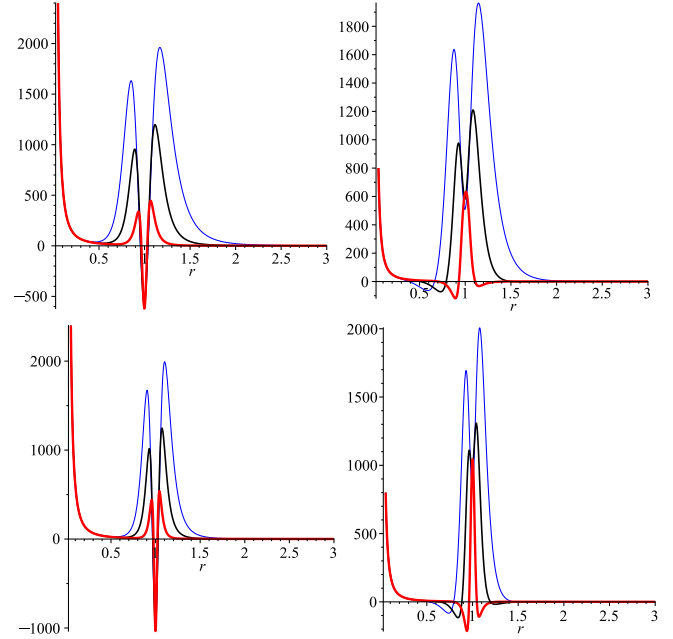
FIG. 2 (color online). Schrödinger-like potentials V^L_{sch} (left) and V^R_{sch} (right) for $\ell = 2$. We fix $r_0 = 1$, and $\eta = 30$. We have (a) $\lambda = 30$ (upper figures) and (b) $\lambda = 50$ (lower figures). In all figures $s = 0.1$ (blue thinner line), $s = 0.15$ (black line), $s = 0.3$ (red thicker line).

zero as $r \to \infty$, indicating the possible presence of resonances. The increasing of η turns the barrier of the potential higher, whereas the increasing of λ turns it thinner. We noted that ℓ influences the behavior of the potential for $r < r_0$ but has no sensible influence on the barrier, and we also observe that the increasing of r_0 turns the potential barrier wider.

Figures 3(a)–3(f) show some results of P_{tube} as a function of m for the left and right fermions. The behavior of P_{tube} is characterized by the presence of some peaks. The thinner the peak, the larger the lifetime of the corresponding resonance. The masses of the resonances for the left and right components are roughly the same (for the parameter used, better than one part in 10^8), as can be seen in the figure. The plots are for $\ell = 2$, $r_0 = 1$, $\eta = 30$ and $\lambda = 30$ and for various values of s. We used $r_{\min} = 10^{-8}$, $r_{\max} = 2$ and step in r equal to $\Delta r = 10^{-3}$. For the mass interval considered we verified that the peak positions do not depend on the choice of $r_{\max} \gtrsim 2$. The plots show several thin peaks of resonances followed by a plateau (value around $P_{\text{tube}} \sim r_0/r_{\max}$) for larger masses $m > m^*$ where m^* is the mass value characterizing the beginning of the plateau. We note that the value of m^* decreases with the increasing of s, reducing the available interval of masses for the possible appearance of resonances. Thus it seems that larger values of s favor the appearing of resonances with lighter masses.

We note that for $s = 0.03$ [Fig. 3(a)] we found no resonance peak. For $s = 0.08$ [Fig. 3(b)] there are more and
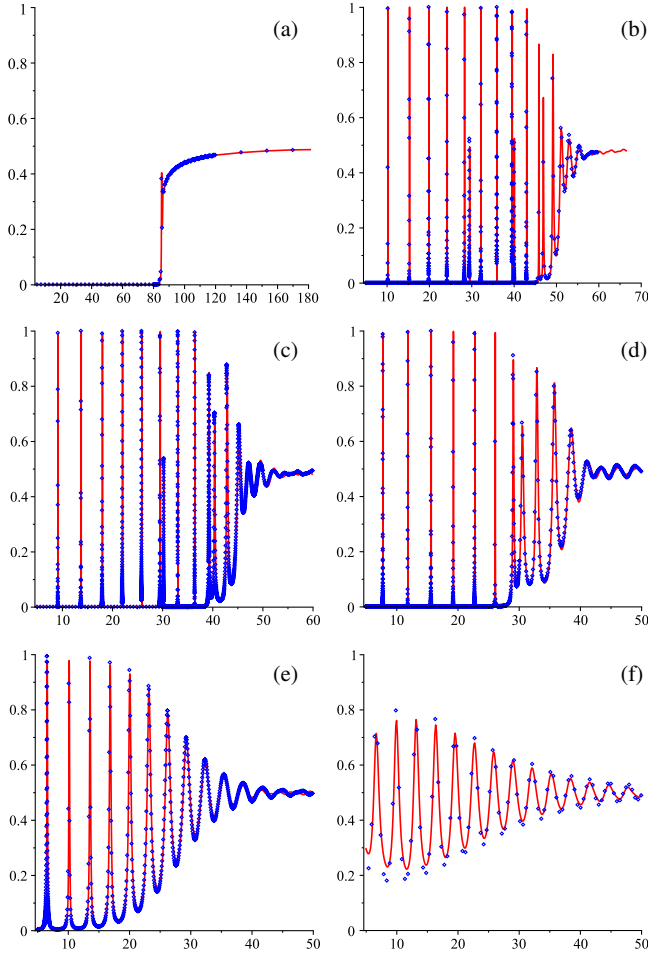
FIG. 3 (color online). P_{tube} as a function of m for the left- (red line) and right-component (blue dots) fermions with $\ell = 2$, $r_0 = 1$, $\eta = 30$, $\lambda = 30$, (a) $s = 0.03$,   (b) $s = 0.08$,   (c) $s = 0.10$, (d) $s = 0.15$, (e) $s = 0.30$, (f) $s = 0.45$.

FIG. 4 (color online). P_{tube} as a function of m for the left- (red line) and right-component (blue dots) fermions with $\ell = 2$, $r_0 = 1$, $\eta = 30$, $\lambda = 30$ and $s = 0.08$ corresponding to a zoom from some peaks of Fig. 3(b).

roughly equally spaced longer-lived resonance peaks, in comparison to $s = 0.10$ [Fig. 3(c)]. The same conclusion applies increasing s to $s = 0.15$ [Fig. 3(d)] and up to $s = 0.30$ [Fig. 3(e)], where now due to their enlargement, the structure of the first peaks is already visible in the scale used in the plot. For $s > 0.30$ we have a less pronounced regime of resonances in comparison to $s = 0.30$, in the sense of the complete loss of resonant character, as seen in Fig. 3(f) for $s = 0.45$.

Note also that for $s = 0.15$ [Fig. 3(d)] and $s = 0.30$ [Fig. 3(e)] the low mass resonances with higher relative probability are more long-lived, which is in accord with results from the literature [24,63–65] obtained in the context of branes. Also, for $s = 0.08$ and $s = 0.10$ [Figs. 3(b) and 3(c)] we have the presence of some peaks with lower relative probability that follows the same pattern when compared separately. As an example we depict in Fig. 4 some plots for $s = 0.08$ corresponding to zooms from some peaks of Fig. 3(b). Note from the figure that the peaks on the right side have $P_{\text{tube}} \sim 1$

whereas the peaks on the left side have lower relative probability $P_{\text{tube}} \sim 0.5$. In this way the results from Refs. [24,63–65] must be interpreted separately for these two sets of peaks.

This can be explained from the discussion of Sec. II. There we saw that lower values of s mean that the influence of the χ field turns out to be more important. From Fig. 1(b) we saw that for $s \gtrsim 0.27$ we have an energy density characteristic of a cylindrical tube. Such energy density is continuously deformed with the reduction of s, and an evident effect of such deformation for $s = 0.08$ and $s = 0.10$ is the loss of a well-organized structure of resonances.

Another important point is that in general the masses of the resonances m_{ress} increase gradually for lower values of s, but the relation $M_{\text{ring}} \ll m_{\text{ress}}$ was always verified, guaranteeing a condition for no backreaction of the fermions in the ring. The larger lifetime of the modes agrees with the correspondingly larger barrier of the Schrödinger-like potential around $r = r_0$ (compare with Fig. 2). This property of V_{sch} is also responsible for the presence of resonance modes, in general, more massive for lower values of s ($s \to \frac{1}{2\lambda}$) which are closely related to the larger influence of the χ field in the internal structure of the defect. However, in this limit the number of the resonances is reduced because the mass values cannot be higher than the tube barrier. In this way, for finding long-lived resonances, there appears to be a physical compromise between a thinner tube (larger values of s which unfavor the presence of the χ field) and the Yukawa coupling $\phi\chi$

(smaller values of s related to a greater influence of the field χ).

V. REMARKS AND CONCLUSIONS

We have studied the localization of $(1 + 1)$-dimensional fermionic fields in a generalized tubelike topological defect whose cross section is a ring constructed with two scalar fields. First, we have considered a general coupling between the defect and the fermion field carefully constructed to provide a supersymmetric quantum-mechanical description of the amplitudes related to the left- and right-fermionic components. Consequently, the Hamiltonians describing such amplitudes are supersymmetric partners forbidding the existence of tachyonic modes. For the Yukawa coupling $F(\phi, \chi) = \eta \phi \chi$ it was shown that the zero mode is non-normalizable and that the spectra of both components are identical due to the spontaneous breaking of supersymmetry. Such result is corroborated by the numerical analysis of the Hamiltonian spectra. Also, it was found that larger couplings η and λ are more effective for finding resonances after a fine-tuning of the constant s characterizing the internal structure of the defect.

As a further comment we would like to point out that the Yukawa coupling is useful for studies of the electromagnetic charge of the ring and some effects like charge fractionalization. These studies are currently under consideration.

[1] K. Akama, Lect. Notes Phys. **176,** 267 (1983).
[2] V. A. Rubakov and M. E. Shaposhnikov, Phys. Lett. **125B,** 136 (1983).
[3] V. A. Rubakov and M. E. Shaposhnikov, Phys. Lett. **B125,** 139 (1983).
[4] K. Akama, in *Proceedings of the Symposium on Gauge Theory and Gravitation, Nara, Japan, 1982*, edited by K. Kikkawa, N. Nakanishi, and H. Nariai (Springer-Verlag, Berlin, 1983).
[5] M. Visser, Phys. Lett. **159B,** 22 (1985).
[6] L. Randall and R. Sundrum, Phys. Rev. Lett. **83,** 3370 (1999).
[7] O. DeWolfe, D. Z. Freedman, S. S. Gubser, and A. Karch, Phys. Rev. D **62,** 046008 (2000).
[8] M. Gremm, Phys. Lett. B **478,** 434 (2000).
[9] M. Gremm, Phys. Rev. D **62,** 044017 (2000).
[10] A. Kehagias and K. Tamvakis, Mod. Phys. Lett. A **17,** 1767 (2002).
[11] C. Csaki, J. Erlich, T. Hollowood, and Y. Shirman, Nucl. Phys. **B581,** 309 (2000).
[12] A. Campos, Phys. Rev. Lett. **88,** 141602 (2002).
[13] R. Guerrero, A. Melfo, and N. Pantoja, Phys. Rev. D **65,** 125010 (2002).
[14] D. Bazeia, C. Furtado, and A. R. Gomes, J. Cosmol. Astropart. Phys. 02 (2004) 002.
[15] D. Bazeia and A. R. Gomes, J. High Energy Phys. 05 (2004) 012.
[16] D. Bazeia, F. A. Brito, and A. R. Gomes, J. High Energy Phys. 11 (2004) 070.
[17] V. Dzhunushaliev, V. Folomeev, and M. Minamitsuji, Rep. Prog. Phys. **73,** 066901 (2010).
[18] R. Jackiw and C. Rebbi, Phys. Rev. D **13,** 3398 (1976).
[19] C. Ringeval, P. Peter, and J.-P. Uzan, Phys. Rev. D **65,** 044016 (2002).
[20] R. Davies and D. P. George, Phys. Rev. D **76,** 104010 (2007).
[21] Y.-X. Liu, C.-E. Fu, L. Zhao, and Y.-S. Duan, Phys. Rev. D **80,** 065020 (2009).
[22] S. L. Dubovsky, V. A. Rubakov, and P. G. Tinyakov, Phys. Rev. D **62,** 105011 (2000).
[23] C. A. S. Almeida, R. Casana, M. M. Ferreira, Jr., and A. R. Gomes, Phys. Rev. D **79,** 125022 (2009).
[24] Y.-X. Liu, J. Yang, Z.-H. Zhao, C.-E. Fu, and Y.-S. Duan, Phys. Rev. D **80,** 065019 (2009).
[25] Y.-X. Liu, H.-T. Li, Z.-H. Zhao, J.-X. Li, and J.-R. Ren, J. High Energy Phys. 10 (2009) 091.
[26] Y.-X. Liu, C.-E. Fu, H. Guo, S.-W. Wei, and Z.-H. Zhao, J. Cosmol. Astropart. Phys. 12 (2010) 031.
[27] W. T. Cruz, A. R. Gomes, and C. A. S. Almeida, Eur. Phys. J. C **71,** 1790 (2011).
[28] C.-E. Fu, Y.-X. Liu, and H. Guo, Phys. Rev. D **84,** 044036 (2011).
[29] Y.-X. Liu, H. Guo, C.-E. Fu, and J.-R. Ren, J. High Energy Phys. 02 (2010) 080.
[30] D. Bazeia, J. Menezes, and R. Menezes, Phys. Rev. Lett. **91,** 241601 (2003).
[31] D. Bazeia, J. Menezes, and R. Menezes, Mod. Phys. Lett. B **19,** 801 (2005).
[32] R. Hobart, Proc. Phys. Soc. London **82,** 201(1963).
[33] G. H. Derrick, J. Math. Phys. (N.Y.) **5,** 1252 (1964).
[34] R. Rajaraman, *Solitons and Instantons* (North-Holland, Amsterdam, 1982).
[35] M. Alford, J. A. Bowers, and K. Rajagopal, Phys. Rev. D **63,** 074016 (2001).
[36] M. G. Alford, K. Rajagopal, T. Schaefer, and A. Schmitt, Rev. Mod. Phys. **80,** 1455 (2008).
[37] R. Casalbuoni, R. Gatto, M. Mannarelli, and G. Nardulli, Phys. Lett. B **511,** 218 (2001).
[38] R. Casalbuoni, R. Gatto, M. Mannarelli, and G. Nardulli, Phys. Rev. D **66,** 014006 (2002).
[39] F. Sannino, N. Marchal, and W. Schäfer, Phys. Rev. D **66,** 016007 (2002).

[40] N. Arkani-Hamed, S. Dimopoulos, G. Dvali, and N. Kaloper, Phys. Rev. Lett. **84**, 586 (2000).

[41] N. Kaloper, Phys. Lett. B **474**, 269 (2000).

[42] P.-M. Ho and Y.-T. Yeh, Phys. Rev. Lett. **85**, 5523 (2000).

[43] O. Bertolami and L. Guisado, J. High Energy Phys. 12 (2003) 013.

[44] R. L. Dobrushin, Theory Probab. Appl. **17**, 582 (1973).

[45] C. Borgs, Commun. Math. Phys. **96**, 251 (1984).

[46] D. Bazeia, M. J. dos Santos, and R. F. Ribeiro, Phys. Lett. A **208**, 84 (1995).

[47] M. A. Shifman and M. B. Voloshin, Phys. Rev. D **57**, 2590 (1998).

[48] A. A. Izquierdo, M. A. Gonzalez Leon, and J. M. Guilarte, Phys. Rev. D **65**, 085012 (2002).

[49] A. de Souza Dutra, A. C. Amaro de Faria, Jr., and M. Hott, Phys. Rev. D **78**, 043526 (2008).

[50] C. Nohl, Phys. Rev. D **12**, 1840 (1975).

[51] H. deVega, Phys. Rev. D **18**, 2932 (1978).

[52] R. Jackiw and P. Rossi, Nucl. Phys. **B190**, 681 (1981).

[53] G. D. Starkman, D. Stojkovic, and T. Vachaspati, Phys. Rev. D **63**, 085011 (2001).

[54] D. Stojkovic, Int. J. Mod. Phys. A **16**, 1034 (2001).

[55] G. Starkman, D. Stojkovic, and T. Vachaspati, Phys. Rev. D **65**, 065003 (2002).

[56] E. Witten, Nucl. Phys. **B249**, 557 (1985).

[57] I. Oda, Phys. Rev. D **62**, 126009 (2000).

[58] M. Gogberashvili and D. Singleton, Phys. Rev. D **69**, 026004 (2004).

[59] E. R. Bezerra de Mello, J. High Energy Phys. 06 (2004) 016.

[60] A. Gangopadhyaya, J. V. Mallow, and C. Rasinariu, *Supersymmetric Quantum Mechanis* (World Scientific, Singapore, 2011).

[61] N. Fernández-García and O. Rosas-Ortiz, Int. J. Theor. Phys. **50**, 2057 (2011).

[62] R. A. C. Correa, A. de Souza Dutra, and M. B. Hott, Classical Quantum Gravity **28**, 155012 (2011).

[63] H.-T. Li, Y.-X. Liu, Z.-H. Zhao, and H. Guo, Phys. Rev. D **83**, 045006 (2011).

[64] H. Guo, Y.-X. Liu, Z.-H. Zhao, and F.-W. Chen, Phys. Rev. D **85**, 124033 (2012).

[65] Q.-Y. Xie, J. Yang, and L. Zhao, Phys. Rev. D **88**, 105014 (2013).